21º POSMEC – Simpósio do Programa de Pós-graduação
UNIVERSIDADE FEDERAL DE UBERLÂNDIA
Faculdade de Engenharia Mecânica
Programa de Pós-graduação em Engenharia Mecânica
www.posgrad.mecanica.ufu.br

ASSESSMENT OF NUMERICAL INTEGRATION SCHEMES APPLIED TO INERTIAL PARTICLE TRACKING IN CYCLONE SEPARATORS

Ricardo de Vasconcelos Salvo, Francisco José de Souza, Diego Alves de Moro Martins

Keywords: Cyclone Separator, LES, Eulerian-Lagrangian, Grade efficiency, Numerical integration schemes

Abstract. Gas-solid flow is extremely important in many industrial branches, since it is found in various operations, which include pneumatic transport, fluidized beds and several industrial pollution control devices, such as cyclone separators. From a numerical point of view there are basically two treatments for gas-solid flow, namely the Eulerian-Eulerian and the Eulerian-Lagrangian approaches. In the former, both the continuous phase (gas flow field) and the particulate phase (solid particles) are treated in an Eulerian reference frame, i.e., it is assumed that the particulate phase can also be treated as a continuum, being more recommended for dense flows. In the second approach, the particulate phase is treated in a Lagrangian reference frame. The individual particles trajectories are computed as ordinary differential equations based on Newton's second law. In order to compute particles velocity and position, these ODEs have to be integrated in time. In the present work, a comparative study between different numerical schemes for integrating these ODEs, namely the Euler scheme, the trapezoidal scheme and an analytical scheme, was performed. The assessment of these integration schemes was performed in an LES simulation (with the dynamic turbulence model) of the flow within a small laboratory cyclone separator, operating at a moderate Reynolds number. The grade efficiency curves are compared to experimental data for each scheme. The numerical code utilized is an in-house tool, UNSCYFL3D, based on the finite volume approach on unstructured grids with the SIMPLE algorithm for pressure-velocity coupling. The results shows that, regardless of the integration scheme, the usage of sub-time steps are mandatory for the integration of particle motion in order to improve results and reduce the cost of the simulations. Also, both the trapezoidal and analytical schemes provide quite similar results, whereas the Euler scheme requires a smaller particle sub-step to ensure accurate solutions.

1 INTRODUCTION

Dispersed particle dynamics are a common issue in many engineering systems, in a way that the need to model and predict the detailed behavior of those flows and the phenomena that they manifest has became a persistent theme throughout the study of multiphase flow. The increase in knowledge of these flows can lead to increases in performance, reduction in cost, and improved safety for these engineering systems. In the past the only ways to obtain this increase was by experimentation through laboratory-sized models equipped with proper instrumentation, and/or theoretically, using mathematical equations and models for the flow (Brennen, 2005; Loth, 2009). Build laboratory scaled plants to study certain types of flow is a good way to obtain the desired information, but normally is a costly process, and its cost may be prohibitive in several applications. To theoretically model complex flows normally requires a great number of simplifications, which can affect the results, and consequently restrict the use of such models to simpler flows. In recent years, Computational Fluid Dynamics (CFD) has become an important tool to help designers to improve their design of single and multiphase systems. In this approach the Navier-Stokes equations and the additional constitutive equations for the other phases are numerically solved providing information on the flow field, and enabling the study of many process variables.

The application of CFD techniques in the simulation of multiphase flow systems requires special attention to the choice of methodologies to be applied on the solution of each phase. This choice results from the compromise between quality of results and computational cost of the

simulation. For the fluid phase, the common practice is to compute it in an Eulerian reference frame, and considering it as being turbulent (as happens in most practical cases). There are basically three main approaches to be considered and those result in three levels of detail and computational cost: a RANS (Reynolds Averaged Navier-Stokes equations) approach where a mean flow field is obtained, as all the space and time scales present in the flow are modeled; a LES (Large Eddy Simulation) where the smallest scales of the flow are modeled, whereas the biggest ones are actually computed, obtaining a time dependent solution, that normally resembles more the actual flow; and by a DNS (Direct Numerical Simulation) where all the flow scales are solved, and the obtained solution, at least from a theoretical point of view, should present the exactly same characteristics of the real flow. Unfortunately, due to its extreme cost, nowadays DNS is still far way from possible for most applications with practical interest. This basically leaves RANS turbulence models or LES turbulence models to be chosen.

Considering the solution of the discrete phase equations, an Eulerian or a Lagrangian reference frame can be used, constituting the so called reference frames: Eulerian-Eulerian and Eulerian-Lagrangian. The Eulerian-Eulerian approach may be sub-divided into mixed-fluid or point-force approaches, in either of the two, both, the fluid and dispersed phase are treated as continuous phases, which makes this approach more suitable for the simulation of dense flows (dense flow in this context is a flow where the overall particle behavior is dictated by particle-particle interactions). The Eulerian-Lagrangian framework can also be further divided into other two approaches: the point-force approach and the resolved surface approach. In both, each computational particle is tracked in the computational domain in a way that it is more suitable for dispersed flows (in this context dispersed flows are those in which the particle movement is dominated by particle-fluid interactions). The Lagrangian resolved surface approach requires much more computational resources, when compared to the Lagrangian point-force approach, since in the former the flow field around the particle has to be well resolved in order to compute the hydrodynamic forces acting over the particle, requiring high cell resolution around each computational particle. In practice this method is only used for a fairly limited number of computational particles (Crowe, 2006).

In the Eulerian-Lagrangian point-force approach, the hydrodynamic forces acting over the particles are calculated by means of theoretical and empirical correlations, e.g., drag coefficient. Normally these relations depend on the particle Reynolds number and/or on phase density ratio; this can lead to some simplifications, e.g., for very light particles (when compared to the carrier fluid) terms associated with the particle density may be neglected, and for very heavy particles many terms associated with the fluid density may be neglected under some circumstances. These simplifications, when possible, contribute to reduce the computational cost.

Our goal is the simulation of gas-solid cyclone separators. When working with abrasive materials these devices normally operate with a low solids volumetric loading, due to the high erosion rate, characterizing a dispersed gas-solid flow. Based on this prior information and on an extensive bibliographic review, the authors decided to use an Eulerian-Lagrangian approach with the point-force approximation coupled with LES modeling of the continuous phase turbulence. The methodology seems promising, but some important issues still remain unexplored: interpolation functions, integrations schemes and subgrid turbulence modulation by the particulate phase. Interpolation functions are necessary because during the computation of particle motion the fluid velocity has to be known at the particle position. Integrations schemes are important because the ordinary differential equations that govern the particles motion have to be integrated over time. Turbulence fluctuation modeling for the particulate phase is a key issue in RANS simulations, since only an average solution is obtained. Although it is an important theme also in LES, it is not as important as in RANS simulations, since at least part of the fluctuations are direct calculated by the simulation. In an attempt to systematically investigate the effect of the abovementioned issues, a comparative study between different numerical integration schemes, namely the Euler scheme, the trapezoidal scheme, and an analytical scheme, was performed in this work. The assessment of these integrations schemes was performed in a simulation of the flow within a small laboratory cyclone separator by comparing the grade efficiency curves to experimental data (R. Xiang, 2001) for each scheme.

2 MATHEMATICAL FORMULATION

2.1 The gas phase

The conservation of mass and the Navier-Stokes equations for a general incompressible linear (Newtonian) viscous flow can be written, adopting the Einstein convention, respectively as:

$$\frac{\partial \rho u_i}{\partial x_i} = 0 \tag{1}$$

$$\frac{\partial \rho u_i}{\partial t} + \frac{\partial}{\partial x_j}\left(\rho u_i u_j\right) = -\frac{\partial p}{\partial x_i} + \frac{\partial}{\partial x_j}\left[\mu\left(\frac{\partial u_i}{\partial x_j} + \frac{\partial u_j}{\partial x_i}\right)\right] \tag{2}$$

By applying a filtering process to the above equations it is possible to separate the larger scales of motion, which are related to the lowest frequencies, from the smallest scales, which are related to the higher frequencies. Equation (2) may be rewritten as:

$$\frac{\partial \rho \overline{u}_i}{\partial t} + \frac{\partial}{\partial x_j}\left(\rho \overline{u_i u_j}\right) = -\frac{\partial \bar{p}^*}{\partial x_i} + \frac{\partial}{\partial x_j}\left[(\mu + \mu_t)\left(\frac{\partial \overline{u_i}}{\partial x_j} + \frac{\partial \overline{u_j}}{\partial x_i}\right)\right] \tag{3}$$

In Eq. (3), the over-bar denotes a filtered quantity, the asterisk denotes the modified pressure, Eq. (4), and μ_t is the turbulent viscosity (this term represents the energy dissipation present on the smallest scales of flow, which are not resolved in LES, so it has to be modeled).

$$\bar{p}^* = \bar{p} + \frac{2}{3}\rho k \tag{4}$$

In Eq. (4), k is the turbulence kinetic energy.

2.2 The dispersed phase

The dispersed phase is treated in a Lagrangian framework, in which each particle is tracked through the domain and its equation of motion is based on Newton's second law. The trajectory equation and the equation of motion in the x-direction for a rigid, spherical particle can be written, respectively, as:

$$\frac{dx_p}{dt} = u_p \tag{5}$$

$$\frac{du_p}{dt} = F_D\left(u - u_p\right) + a \tag{6}$$

Similar equations can be written for the other directions. In Eq. (6) the first term on the right hand side is the drag force experienced by the particle, F_D, given by Eq. (7) and "a" is the acceleration term, which in the present work considers only the gravitational and buoyancy forces – Eq. (8):

$$F_D = \frac{18\mu}{\rho_p d_p^2}\frac{C_D Re_p}{24} \tag{7}$$

$$a = \frac{g(\rho_p - \rho)}{\rho_p} \tag{8}$$

In Eq. (7), Re_p and C_D are the particle Reynolds number, Eq. (9), and the drag coefficient, Eq. (10), respectively:

$$Re_p \overset{\text{def}}{=} \frac{\rho d_p |u_p - u|}{\mu} \tag{9}$$

$$C_D = \begin{cases} 24\,(1 + 0.15Re^{0.687})/Re & Re \leq 1000 \\ 0.44 & Re > 1000 \end{cases} \tag{10}$$

In the above equations, the subscript "p", denotes a discrete phase variable, and the continuous-fluid properties are interpolated to particle center of mass. The drag coefficient, Eq. (10), follows the model proposed by Schiller and Naumann (1935).

3 TURBULENCE MODELS

The flow field within a cyclone separator is extremely complex, displaying strong swirl and consequently highly anisotropic turbulence. Moreover, the motion of the particulate phase is largely controlled by turbulence fluctuations. These fluctuations are responsible to move larger particles toward the cyclone center, allowing some to escape, and smaller particles toward the cyclone wall, promoting the separation of small size particles. According to Hoffman and Stein (2008); Derksen (2003); Derksen (2006) and Derksen (2008), turbulence is one of the most important factors acting over the cyclone separation mechanism. Thus, the correct turbulence modeling is of fundamental importance in the simulation of such devices. Aiming at a precise turbulence modeling, the LES methodology with the dynamic Smagorinsky model was utilized. In this model the eddy viscosity coefficient is locally calculated to reflect closely the state of the flow. This is done by sampling the smallest resolved scales and using this information to model the sub-grid scales (Germano et al., 1990). According to Silveira-Neto (2002), two different filters are utilized:

- The grid filter, in which the grid dimensions are used to calculate its characteristic length.
- The test filter, in which a multiple of grid size, normally two, is used to calculate the characteristic length.

A brief summary of the formulation used in this model for incompressible flows, with the modifications proposed by Lilly (1991), is presented below:

$$C = \frac{1}{2}\left(\frac{L_{ij} M_{ij}}{M_{ij}^2}\right) \tag{11}$$

where:

$$M_{ij} = \left(\tilde{\bar{\Delta}}^2 |\tilde{\bar{S}}| \tilde{\bar{S}}_{ij} - \left(\bar{\Delta}^2 \widetilde{|\bar{S}|\bar{S}_{ij}}\right)\right), \text{ and, } L_{ij} = T_{ij} - t_{ij} \tag{12}$$

and the tensors are defined as:

$$T_{ij} = \left(\widetilde{\bar{u}_i \bar{u}_j}\right) - \tilde{\bar{u}}_i \tilde{\bar{u}}_j, \text{ and, } t_{ij} = \overline{u_i u_j} - \bar{u}_i \bar{u}_j \tag{13}$$

The turbulent viscosity, which is used in the RHS of Eq. (3), is defined as:

$$\mu_t = \rho(C\Delta^2)\bar{S} \tag{14}$$

where Δ is the grid filter length and $\bar{S}$ is the shear strain rate:

$$\bar{S} = \sqrt{S_{ij} S_{ij}}, \text{ and, } S_{ij} = \frac{1}{2}\left(\frac{\partial u_i}{\partial x_j} + \frac{\partial u_j}{\partial x_i}\right) \quad (15)$$

In the above equations the over bar denotes the grid filter process while the over tilde denotes the test filter process.

The model parameter produced by Eq. (11) is a rapidly varying function of spatial coordinates and time so the eddy viscosity may take large values of both signs. This can and does lead to numerical divergence, so a usual technique is clip the negative turbulence viscosity. For more information about this model the interested reader is referred to the original paper presented by Germano (Germano et al, 1990) and the work of Lilly (1991).

Another important factor in the utilization of a LES turbulence model relies in the fact that less stochastic modeling is required since the most containing eddies are resolved explicit. This reduces the importance of the subgrid modeling for the particulate phase. In the present work the subgrid scales were not considered for the particulate phase.

4 NUMERICAL METHOD

4.1 Numerical code

For the simulations, the computational code UNSCYFL3D (Unsteady Cyclone Flow – 3D), was used. This in-house tool was developed as a dedicated tool for simulating highly rotational flows, aiming at the study of cyclones/hydrocyclones and swirl tubes. It is based on the finite volume method in unstructured three-dimensional grids, which enables the faithful representation of complex geometries. The SIMPLE (Semi-Implicit Method for Pressure-Linked Equations) algorithm is used for the velocity-pressure coupling. In all the simulations accomplished in this work the time-advancement was second-order and the central differencing scheme was employed for the advective and diffusive terms of the momentum equations. This numerical scheme does not suffer from the numerical dissipation common, for instance, in the 1º and 2º order UPWIND schemes, in a way that it may lead to numerical instabilities case the Reynolds number is too high and mesh resolution is inadequate. The UNSCY3D does not use any type of artificial dissipation to ensure stability, although it uses the deferred correction scheme, which helps to deal with instabilities that may rise from the CDS scheme.

The non-smoothness of the grid and non-orthogonality effects are also taken into account (Ferziger and Peric, 2002). For the solution of the linear systems the biconjugate gradient (Ferziger and Peric, 2002) and the algebraic multigrid (Notay, 2008) methods are used. For the dispersed phase, each particle is tracked in a Lagrangian framework by the particle-localization algorithm proposed by Haselbacher et al. (2007). This algorithm is based on tracking down a particle along its trajectory by computing the intersections of the trajectory and the cell faces, as shown in Fig. 1(a).

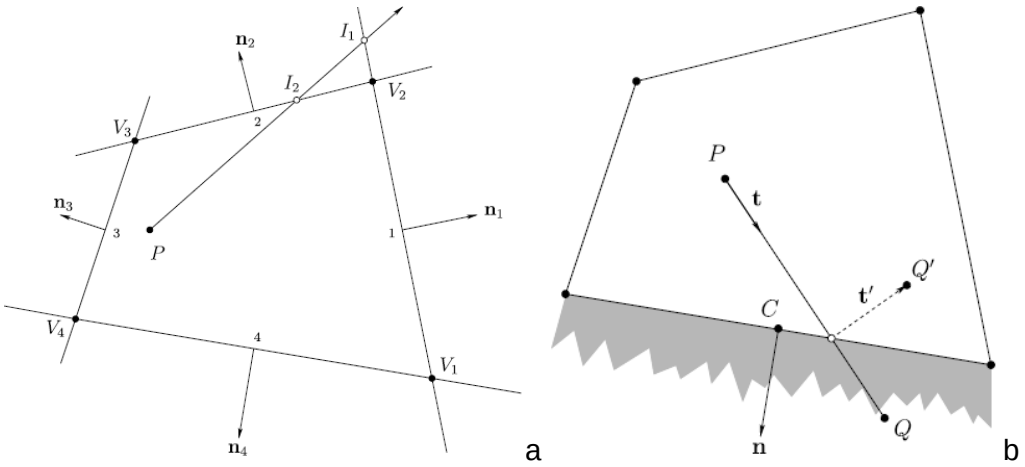

Figure 1: Illustration of how the particle-localization algorithm proposed by Haselbacher et al.

(2007) works, (a) for internal elements and (b) for boundaries. In this figure “n” are the normal vectors, “v” are the element vertices, “t” the trajectory, “ t’ ” the modified trajectory (due to a collision), and “I” are the intersection points, “P” is the particle. Adapted from Haselbacher et al. (2007).

It has some great advantages over other particle-localization algorithms: first, it can be applied to grids consisting of polyhedral cells. Second, the algorithm is not limited to small particle displacements. Third, the interactions of particles with boundaries are dealt in a natural way, Fig. 1(b). Fourth, the algorithm is more efficient than other published algorithms (Haselbacher et al., 2007). Another great advantage is that it is based on “intersection distances” and not on “intersection time” as it is found for a great number of other published algorithms.

Besides that, three different integrations schemes for time advance of the dispersed phase were implemented and tested: the Euler implicit scheme; the trapezoidal scheme; and an analytical scheme.

4.1.1Euler implicit scheme

In the Euler implicit scheme the derivative on the LHS of Eq. (6) is approximated by:

$$\frac{du_p}{dt} = \frac{u_p^{n+1} - u_p^n}{\Delta t} \tag{16}$$

Substituting Eq. (16) in Eq. (6) and manipulating mathematically, yields:

$$u_p^{n+1} = \frac{u_p^n + \Delta t\left(a + \frac{u^{n+1}}{\tau_p}\right)}{\left(1 + \frac{\Delta t}{\tau_p}\right)} \tag{17}$$

where Eq. (17) is the implemented equation of motion for this scheme. For determining the particle position, the trapezoidal scheme is used, Eq. (20).

4.1.2Trapezoidal scheme

The trapezoidal rule is a simple average of the backward-Euler and the forward-Euler schemes. The general form of the trapezoidal rule may be written as:

$$\int_a^b f(x)dx = (b-a)\frac{f(a)+f(b)}{2} \tag{18}$$

Applying Eq. (18) to Eq. (6) and isolating the particle x-velocity at the nest time results in:

$$u_p^{n+1} = \frac{u_p^n\left(1 - \frac{\Delta t}{2\tau_p}\right) + \frac{\Delta t}{2\tau_p}\left(u^n + u^{n+1}\right) + a\Delta t}{\left(1 + \frac{\Delta t}{2\tau_p}\right)} \tag{19}$$

The trajectory equation is obtained by the same procedure.

$$x_p^{n+1} = x_p^n + \Delta t\frac{\left(u_p^n + u_p^{n+1}\right)}{2} \tag{20}$$

4.1.3 Analytical scheme

The particle equations of motion were combined with the particle trajectory equation, Eq. (4), and analytically integrated, assuming that drag force, fluid velocity and acceleration are constant during the particle time step. While this might sound as a brutal simplification, it is a reasonable approximation if the time step is small, which is typically used in LES and required when dealing with small Stokes numbers. The resulting equations for the x-direction, Eq. (21) and Eq. (22) were implemented.

$$u_p^{n+1} = u^n + e^{-\Delta t/\tau_p}\left(u_p^n - u^n\right) - a\tau_p\left(e^{-\Delta t/\tau_p} - 1\right) \quad (21)$$

$$x_p^{n+1} = x^n + \Delta t\left(u^n + a\tau_p\right) + \tau_p\left(1 - e^{-\Delta t/\tau_p}\right)\left(u_p^n - u^n - a\tau_p\right) \quad (22)$$

In the above equations, x_p is the particle position vector; "a" is the acceleration term, given by Eq. (8); τ_p is the particle relaxation time, given by $1/F_D$, where F_D is the drag force defined in Eq. (7); the subscript "p" denotes particle, the superscript "n+1" denotes the calculated variable at the new time step and the superscript "n" denotes the calculated variable at the previous time step.

Currently, two drag models are implemented for spherical particles; the Morsi and Alexander (1972) drag model and the one proposed by Schiller and Naumann (1935). The last one was used in the simulations shown here.

4.2 Numerical procedure

The cyclone geometry simulated is a small sampling cyclone, as shown in Fig. 2 and in Table 1. This is the same geometry experimentally studied by R. Xiang et al. (2001) and numerically simulated by Chuah et al. (2006). The fluid is treated as air with constant density 1.205 Kg/m³ and viscosity 1.82E-05 Kg/m.s. Initially, a steady case for the single phase flow was solved with the SST turbulence model, using a first order upwind scheme, UDS (Ferziger and Peric, 2002), for the conservation equations and convergence criteria of 1.0E-05. The resulting flow field was then used as an initial field for the transient, LES simulations. All the LES simulations were performed with the central-difference scheme for the conservation equations and a convergence criterion of 1.0E-04, with a time step of 1.0E-05 s.

The average residence time for this cyclone is approximately 0.1 s. In order to guarantee that a statistically established regime had been reached, 0.5 s of physical time were simulated prior to the particle injection. Then the last instantaneous field was used as an initial field for the gas-solid simulations. As for the solid phase, monodisperse polystyrene latex (PSL) particles with density 1050 kg/m³ and diameters 0.5, 1.0, 1.5, 2.0, 2.5, 3.0, 3.5, 4.0, 4.5, 5.0, 5.5, 6.0 μm were simulated.

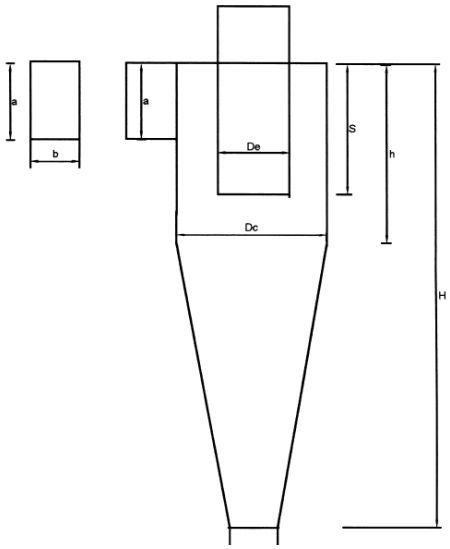

Figure 2: Schematic diagram of the simulated cyclone, adapted from R. Xiang et al. (2001)

Table 1: Geometrical dimensions of the simulated cyclone

Dimension	Lenght (m)	Dimension ratio (dimension/Dc)
Body diameter, Dc	0.031	1
Gas outlet diameter, De	0.0155	0.5
Inlet height, a	0.0125	0.4
Inlet Width, b	0.005	0.16
Cyclone height, H	0.077	2.5
Cylinder height, h	0.031	1
Gas outlet duct lenght, S	0.0155	0.5
Cone botton opening, B	0.0194	0.625

In this work, the wall thickness of the vortex finder was assumed to be D/12.4, since no reference was found for it.

It was found that the LES coupled with the Lagrangian particle tracking is expensive, because the flow must be computed at each time step. Although the particle tracking procedure was found to be rather fast and efficient, the whole calculation up to the time when all the particles have either been collected or escaped takes very long, since several residence times are needed due to the small particle diameters involved. The particle Stokes number, calculated with Eq. (23), and the particle relaxation time, calculated with Eq. (24), are shown in Table 2 as a function of the particle diameter.

$$St = (\rho_s - \rho)\frac{d_p^2 U_{in}}{18\mu D_c} \tag{23}$$

$$\tau_p = \frac{\rho_s d_p^2}{18\mu} \tag{24}$$

Particles with larger relaxation times, on the other hand, are quickly directed towards the wall as son as they penetrate the cyclone body.

The particle relaxation time is associated with the time it takes for a particle to respond to a change in the flow. A massless particle, for instance, responds instantaneously to any change in the flow, and thus has the same local velocity as the fluid. As shown in several publications, the flow in a cyclone displays strong upward and downward fluid streams, in which the particles with the lowest relaxation times tend to remain while they are not collected or do not escape through the overflow. Particles with larger relaxation times, on the other hand, are quickly directed towards the wall as soon as they penetrate the cyclone body. Although the carrier flow velocity is low in the near-wall region because of the boundary layer, normally a 100% of these particles reach the cyclone bottom after a few residence times, and are then considered collected. From the experiments by R. Xiang et al. (2001), it is known that particles larger than 4.5 micrometers are collected with nearly a 100% grade efficiency in this cyclone, under the conditions tested.

Table 2: Particle Stokes number and particle relaxation time for the diameters investigated.

Particle diameter (m)	Particle Stokes Number	Particle Relaxation Time (s)
5.00E-07	2.75E-04	8.01E-07
1.00E-06	1.10E-03	3.21E-06
1.50E-06	2.48E-03	7.21E-06
2.00E-06	3.66E-03	1.28E-05
2.50E-06	6.89E-03	2.00E-05
3.00E-06	9.92E-03	2.88E-05
3.50E-06	1.35E-02	3.93E-05
4.00E-06	1.76E-02	5.13E-05
4.50E-06	2.23E-02	6.49E-05
5.00E-06	2.75E-02	8.01E-05
5.50E-06	3.33E-02	9.70E-05
6.00E-06	3.97E-02	1.15E-04

4.3 Boundary Conditions

Boundary conditions for the gas phase:

- At the inlet a normal, uniform velocity profile (U_{in}) of 10.667 m/s, yielding a Reynolds number of approximately 22,000, was used;
- At the overflow outlet the static pressure was prescribed;
- All the cyclone walls were considered as no-slip boundaries;
- The gas was not allowed to leave the cyclone through the underflow (cone bottom).

Boundary conditions for the solid phase:

- The particles were injected with the same velocity as the fluid at the inlet faces (one particle of each diameter in each inlet face center). As the simulations were performed with one-way coupling, the injection was not made continuously (only a particle pulse was utilized for each simulation). The total number of particles injected into the cyclone was 5,100 in each one of the simulations;
- At the wall particles were reflected considering a perfectly elastic collision;
- Particles that touched the cone bottom were considered as collected and particles that crossed the overflow exit were considered escaped and deleted from the calculation.

4.4 Numerical grid

A mesh with approximately 800,000 hexahedral elements, which can be seen in Fig. 3, was used. This mesh was generated with the commercial mesh generator ICEM-CFD. Although automatic generation is possible, this should be avoided when performing LES simulations, since it can lead to non-orthogonal elements, which are more diffusive. In fact, a major concern when constructing the mesh is to made the elements as orthogonal to each other as possible, as can be seen in Fig. 4.

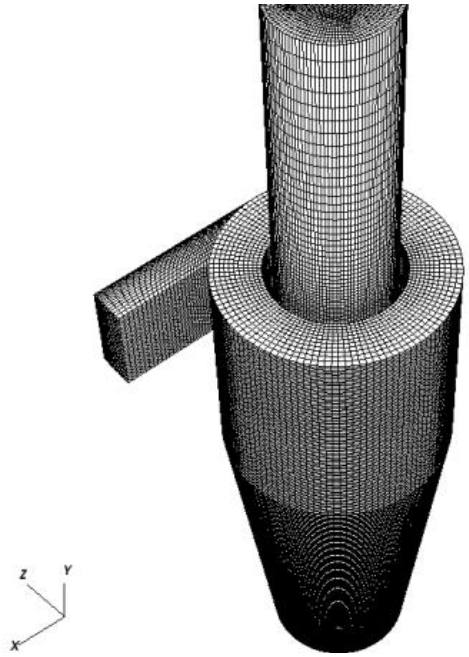

Figure 3. Hexahedral mesh with approximately 800,000 elements used in all the simulations.

Figure 4 also show that there is no concern to y+ when constructing the mesh, previous studies showed that boundary layer refinement in cyclone simulations was not advantageous, mainly for two reasons:

- the number of elements near the wall becomes excessive, making it necessary to reduce the number of elements in the central region, which is the region with higher turbulence intensity;
- The stretching becomes excessive in boundary layer elements.

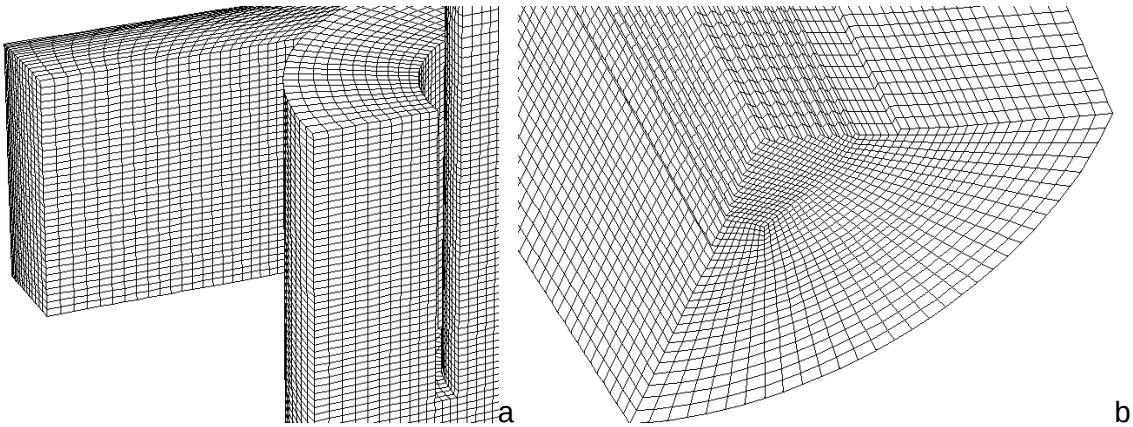

a b

Figure 4. Mesh details. a). cylindrical part of the cyclone. b). cyclone cone apex.

5 RESULTS

The three schemes for the temporal integration of the particle equations of motion were tested, and their influence on the grade efficiency of the cyclone was analyzed. Because the grade efficiency can be seen as the result of a set of variables, and as such, carries many uncertainties and depends strongly on many parameters, it is not a good figure of merit for the quality of numerical schemes. Ideally, we would like to compare the results for the flow field as well as the particle trajectories for some diameters in a well-known cyclone geometry. Nevertheless, references containing all this information regarding the fluid and particle flow for the same cyclone geometry are rare, so that the validation of the single phase results was done in previous

publications, Salvo (2009); Salvo et al. (2010); Salvo et al. (2011). It is believed that the flow field for this cyclone is accurately calculated.

Because the particle diameters are in the order of a few micrometers, the Stokes numbers involved are consequently very small, as presented in Table 2. This in turn requires small time steps, which might be even lower than that used for the LES of the fluid flow. A study on the usage of time sub-steps for the dispersed phase was then accomplished. The results are presented below, which initially show the importance of using subtime steps for each integration scheme, and then a direct comparison of the different schemes is presented.

In these tests, the fluid flow time step was kept constant and equal to 10^{-05} s. As for the particle tracking, numerical experiments were run with 1, 2 and 4 steps, corresponding to particle time steps of 10^{-05}, $5x10^{-06}$ s and $2.5x10^{-06}$ s, respectively. From Figs. 5, 6 and 7, it can be clearly noted that the smaller the order of convergence of the method used, the greater is the influence of the use of sub-time steps, as expected. The analytical scheme is seen to be the least sensitive to the particle time step.

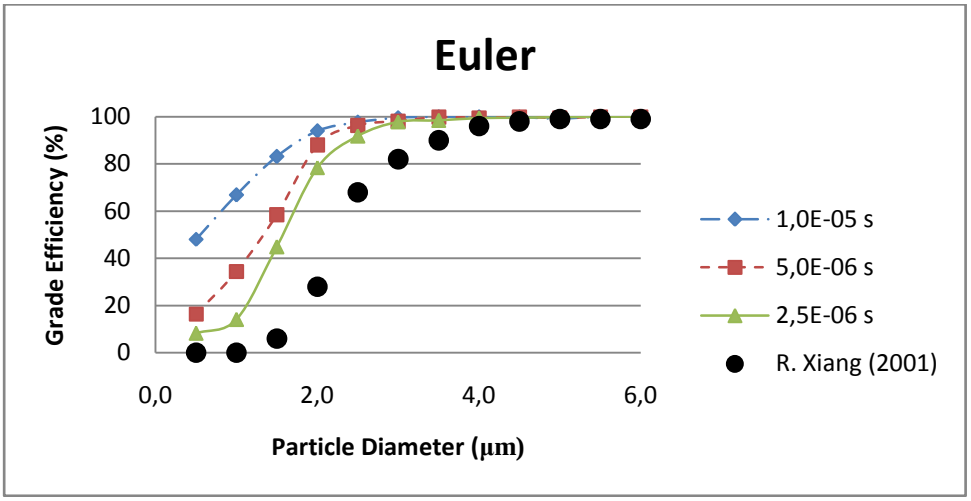

Figure 5: Influence of the time step for the particulate phase while using the Euler implicit scheme. The time step for the fluid phase was kept constant at 10^{-05} s.

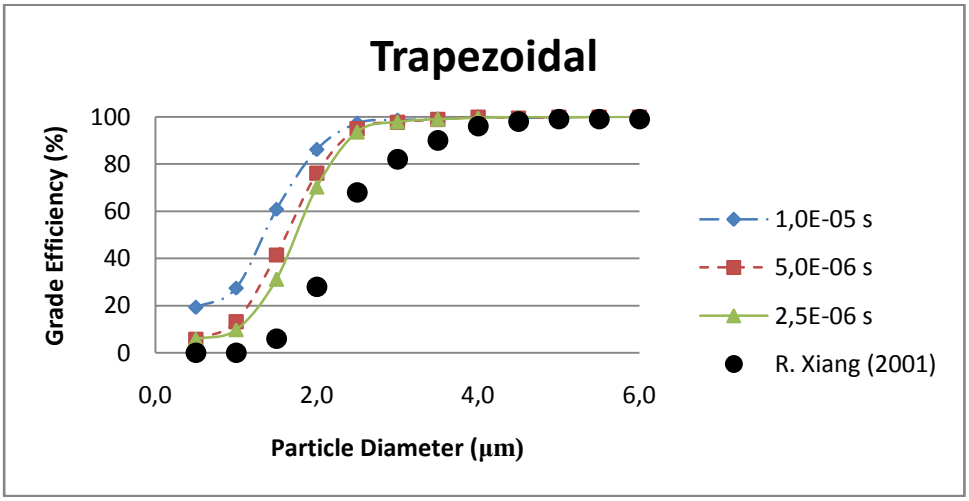

Figure 6: Influence of the time step for the particulate phase while using the Trapezoidal scheme. The time step for the fluid phase was kept constant at 10^{-05} s.

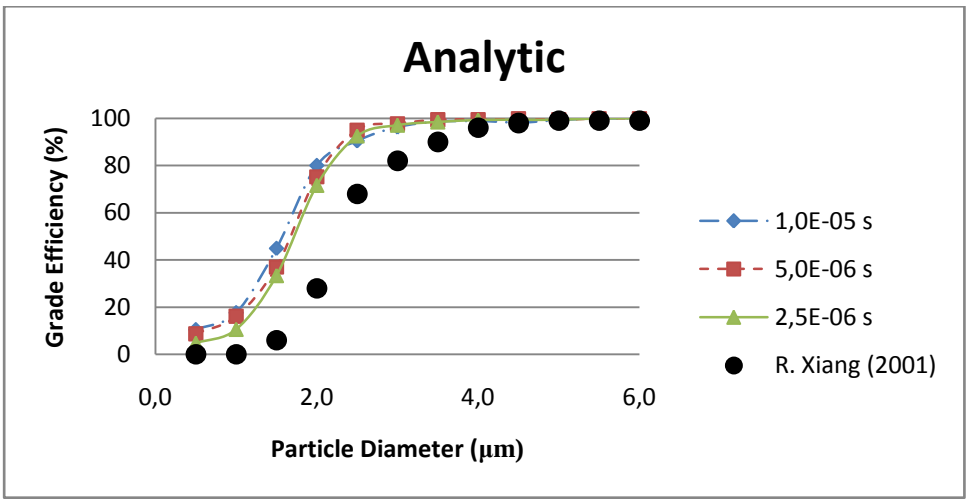

Figure 7: Influence of the time step for the particulate phase while using the Analytic scheme. The time step for the fluid phase was kept constant at 10^{-05} s.

For the purpose of comparing all the integration methods, the same data presented in Figs. 5, 6 and 7 is shown below, enabling a direct comparison between the different integration schemes with four time sub-steps (time step of $2.5x10^{-06}$ s for the particulate phase). It is easy to see that, based on the experimental data, the best results are obtained with the analytical integration scheme, followed very closely by the trapezoidal scheme. Results for more than 4 sub-time steps were run, but are not shown below because the grade efficiency curves collapse, indicating that results are "Δt converged" and seen not to depend on the integration method anymore.

Besides improving accuracy, another great advantage of using sub-time steps is that the computational cost is considerably reduced, since the fluid flow calculation is done less frequently.

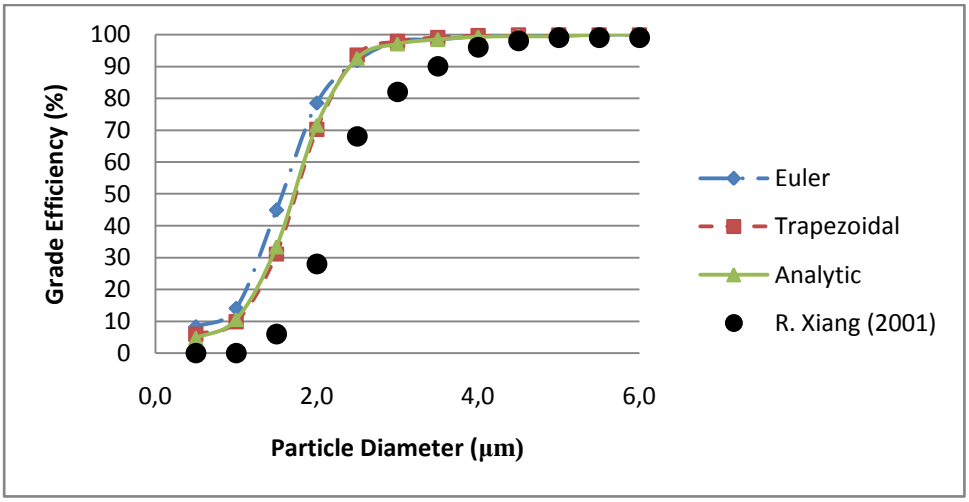

Figure 8. Direct comparison between the results obtained with the different integration schemes using a time step of 10^{-05} s for the fluid phase and $2.5x10^{-06}$ s for the particulate phase.

Obviously, there are other important issues to be regarded with respect to the agreement between the simulated and experimental collection curves, such as the spatial resolution of the Eulerian mesh. The Stokes number represents the ratio particle relaxation time over the fluid characteristic time. Therefore, a low Stokes number means that the particles is sensitive to the small turbulence scales, possibly those which have not been captured in the current simulation. In a previous study, it was observed that refining the mesh from 380,000 elements to nearly 800,000 elements brought the numerical grade efficiency curve closer to the experimental one, so a mesh independence test still has to be done (there are some simulations in course with a 1,800,000 elements mesh), which might hopefully reduce such disparity.

Another critical issue is the turbulence modeling for the fluid phase. A previous investigation, Salvo et al. (2011) showed that differences on RMS profiles generated by different

turbulence models might lead to considerable differences in the numerical grade efficiency curve Salvo et al. (2011).

As far as the time integration method for the particles is concerned, it can be concluded that the sub-time steps must be used, regardless of the integration method, if accurate results are sought.

6 CONCLUSIONS

The simulation of small laboratory cyclone operating at a moderate Reynolds number was performed. In those simulations the dynamic sub-grid model was utilized in an Eulerian-Lagrangian reference frame and three different temporal integrations schemes for the particulate phase were assessed through the comparison between numerically obtained grade efficiency curves and experimental ones. The influence of the use of sub-time steps was also verified, and the main conclusions to be drawn from the results presented above are:

- The temporal integration scheme does affect the grade efficiency curves. But, as the time step becomes vanishing small, this influence tends to zero;
- The use of sub-time steps for the particulate phase is a good option, if not a necessary one, once it may offer the opportunity of simulate the fluid phase, which is the most expensive part (at least in one-way simulations) with higher time steps, providing an enormous economy of resources.

Another important factor that has to be considered is the turbulence modeling for the fluid phase, which may strongly affect the results.

Acknowledgments

The authors would like to thank: FAPEMIG, CAPES and PETROBRAS for the financial support.

REFERENCES

Brennen, C. E. *Fundamentals of multiphase flow*. Cambridge University Press, 2005.

Chuah, T.G., Gimbun, J. and Choong, T.S.Y. A CFD study of the effect of cone dimensions on sampling aerocyclones performance and hydrodynamics. *Power Technology*, 162:126-132, 2006.

Crowe, T. C. *Multiphase flow handbook.* CRC, 2006.

Derksen, J.J. Separation performance predictions of a Stairmand high-efficiency cyclone. *Fluid Mechanics and Transport Phenomena*, 49:1359-1371, 2003.

Derksen, J.J., van den Akker, H.E.A. and Sundaresan, S. Two-way coupled Large-Eddy simulations of the gas-solid flow in cyclone separators. *American Institute of Chemical Engineers*, 54:872-884, 2008.

Derksen, J.J., Sundaresan, S. and van den Akker, H.E.A. Simulation of mass-loading effects in gas-solid cyclone separators. *Power Technology*, 163:59-68, 2006.

Ferziger, J.H. and Peric, M. *Computational methods for fluid dynamics*, Springer, 2002.

Germano, M., Piomelli, U., Moin, P. and Cabot, W.H. A dynamic subgrid-scale eddy viscosity model. *American Institute of Physics*, 7:1760-1795, 1990.

Haselbacher, A., Najjar, F.M. and Ferry, J.P. An efficient and robust particle-localization algorithm for unstructured grids. *Journal of Computational Physics*, 225:2198-2213, 2007.

Hoekstra, A.J., Derksen, J.J. and Van den Akker, H.E.A. An experimental study of turbulent swirling flow in gas cyclones. *Chemical Engineering Science*, 54:2055-2065, 1999.

Hoffman, A.C., Stein, L.E. *Gas cyclones and swirl tubes – principles, design and operation.* Second Edition, Springer – Verlag Berlin Heidelberg, 2008.

Lilly, D. K. A proposed modification of the Germano subgrid-scale closure method. *Physics Fluids*, 4:633-635, 1992.

Loth, E. *Computational fluid dynamics of bubbles, drops and particles*. Cambridge University Press, 2009.

Morsi, S.A. and Alexander, A.J. An investigation of particle trajectories in two-phase flow systems, *J. Fluid Mech.*,1972, 55:193-208.

Notay, Y. An aggregation-bases algebraic multigrid method, *Electronic transactions on numerical analysis*, 37:123-146, 2010.

Salvo, R. V. *Efeitos de modelos submalha em escoamentos em ciclones.* Dissertation, FEMEC, Universidade Federal de Uberlândia, Uberlândia, Brasil, 2009.
Salvo, R. V., Souza, F. J., Martins, D. A. M. and Silveira-Neto, A. Comparison between different large eddy turbulence models in the simulation of single phase flows in a cyclone, *13th Brazilian Congress of Thermal Science and Engineering*, Uberlandia, Brazil, 2010.
Salvo, R. V., Souza, F. J. and Martins, D. A. M. LES and DES simulations of particle paths inside a small sampling cyclone separator, 2011.
Salvo, R. V., Souza, F. J. and Martins, D. A. M. Analysis of sub-grid modeling effects in the simulation of the single-phase turbulent flow in na industrial cyclone separator, 2011.
Silveira-Neto, A. 2002., Turbulência nos Fluidos Aplicada. Apostila do curso de pós-Graduação em Engenharia Mecânica da Universidade Federal de Uberlândia.
Schiller, L. and Naumann, Z. Deutsch. Ing., 77:318, 1935.
Xiang, R., Park, S.H. and Lee, K.W. Effects of cone dimension on cyclone performance. *Journal of Aerosol Science*, 32:549-561, 2001.